ACS Macro Letters

Letter

pubs.acs.org/macroletters

Synthesis of Amphiphilic Naturally-Derived Oligosaccharide-*block*-Wax Oligomers and Their Self-Assembly

Julia D. Cushen,[†] Kadhiravan Shanmuganathan,[†] Dustin W. Janes,[†] C. Grant Willson,[†,‡] and Christopher J. Ellison*[,†]

[†]McKetta Department of Chemical Engineering, The University of Texas at Austin, Austin, Texas 78712, United States

[‡]Department of Chemistry, The University of Texas at Austin, Austin, Texas 78712, United States

Supporting Information

ABSTRACT: Self-assembly characteristics of amphiphilic macromolecules into micelles, nanoparticles and vesicles has been of fundamental interest for many applications including designed nanoscale therapeutic delivery systems and enzymatic reactors. In this work, a class of amphiphilic block oligomers was synthesized from naturally occurring oligosaccharides and aliphatic alcohol precursors, which are all currently prominent in the pharmaceutical, food, and supplement industries. These block oligomer materials were synthesized by functionalization of the precursor materials followed by subsequent coupling by azide−alkyne cycloaddition and their bulk self-assembly was investigated after solvent vapor annealing. Self-assembly of the amphiphilic materials into liposomes in aqueous solution was also investigated after preparing solutions using a nanoprecipitation method. Encapsulation of hydrophobic components was demonstrated and verified using dynamic light scattering, transmission electron microscopy, and fluorescence spectroscopy experiments.

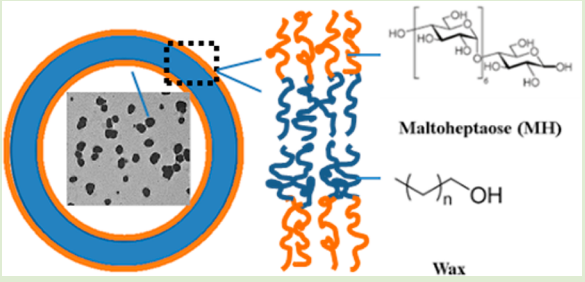

In recent years, there has been tremendous interest in developing functional materials and composites based on naturally derived feed stocks. While natural polymers such as cellulose, chitin, and polypeptides are being explored for advanced medical and electronic applications,[1−3] there is also an increased demand for conversion of biobased feed stocks into viable macromolecular structures.[4] Apart from economic and environmental benefits, properties such as biocompatibility, biodegradability, and low toxicity that most often accompany these biobased polymers make them attractive for potential applications in medical diagnostics, therapeutics, and food packaging. However, to facilitate the penetration of biobased polymers into niche markets, it is imperative to take advantage of new synthetic tools such as controlled living polymerization and click chemistry to precisely design structurally intriguing macromolecular architectures. To this end, we report here on the synthesis and self-assembly behavior of amphiphilic block oligomers that are completely based on edible, naturally derived precursor molecules, namely, oligosaccharide and wax. In related recent reports, sugar-based hybrid copolymers have been pursued, wherein one block of the copolymer is still petroleum-based.[5,6] We believe that amphiphilic macromolecules that are completely naturally derived have their own advantages, and an effort to synthesize and characterize such biobased amphiphiles will enrich their design and scope.

Amphiphilic macromolecules are an important class of materials that can be used as core−shell nanoscale delivery systems,[7,8] as surfactants for solubilizing drugs,[9] and in a wide variety of other applications.[10] Due to the chemical dissimilarity of the blocks and the typical affinity of one block for a particular solvent, amphiphilic macromolecules can self-assemble into structures such as micelles or vesicles (e.g., polymersomes) in solution,[11,12] much like naturally occurring surfactants and lipids.[13] Polymersomes are comprised of bilayers of amphiphilic macromolecules, where the hydrophobic blocks of each molecule associate with each other occupying the middle part of the vesicle "wall" and the hydrophilic blocks are exposed to the inner and outer aqueous environment. The ability to alter the composition and molecular weight of the blocks allows preparation of polymersomes of much larger bilayer thickness (up to 40 nm) as compared to liposomes (ca. 4 nm), yielding better solubility of hydrophobic molecules and mechanical stability as carrier systems.[14] Akin to biological vesicles comprised of amphiphilic lipids, which incorporate cholesterol and membrane proteins, liposomes derived from natural feed stocks could serve as a reservoir for hydrophobic and amphiphilic molecules. In this report, we investigated the self-assembly behavior of oligosaccharide-*block*-wax amphiphiles into vesicles and their ability to encapsulate hydrophobic molecules.

Three amphiphlic block oligomers were synthesized from naturally occurring, nontoxic precursor materials that are already approved for human consumption and currently have uses in the pharmaceutical, food, and nutritional supplement industries. The precursor materials consisted of functionalized hydrophilic

Received: June 27, 2014
Accepted: August 1, 2014
Published: August 11, 2014

   dx.doi.org/10.1021/mz500389g | *ACS Macro Lett.* 2014, 3, 839−844

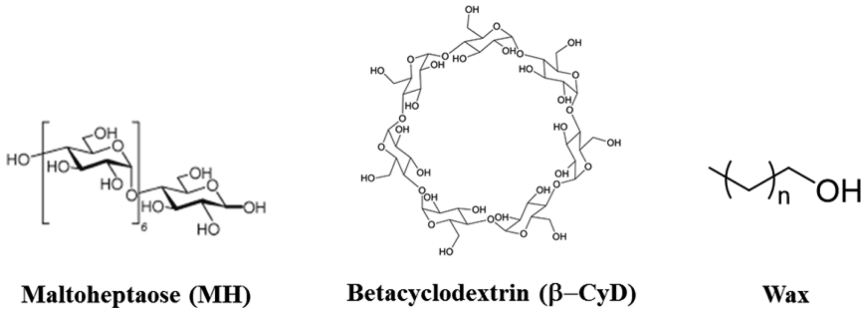

Figure 1. Chemical structures of the block precursors used to make the oligosaccharide-*b*-wax amphiphiles.

oligosaccharides and functionalized hydrophobic straight chain alkanes. The three block precursor components used to make the amphiphilic block oligomer materials described in this work are shown in Figure 1. Maltoheptaose (MH) is prepared by enzymatic ring-opening of betacyclodextrin (*β*-CyD),[15] which is produced by enzymatically modifying starches,[16] and both MH and *β*-CyD have uses in the food and pharmaceutical industries.[15,17,18] The aliphatic alcohols used in this work were 1-octacosanol and policosanol, both containing a hydroxyl functionality at their end to enable functionalization. Policosanol is a mixture of primary straight chain aliphatic alcohols with chain lengths ranging from 20 to 36 carbons.[19] Both waxes are isolated from plant sources[19,20] and are currently used as nutritional supplements.[21,22]

Azide–alkyne cycloaddition, a common "click" chemistry strategy, is a versatile coupling technique that has been used previously to combine similar alkyne and azide-functionalized components.[23,24] The oligosaccharides were functionalized with an alkyne, the aliphatic alcohols were azide-functionalized, and the two components were coupled. The materials produced (see Table 1 for a summary) are therefore derived from biorenewable,

Table 1. Sample Abbreviations with the Corresponding Oligosaccharide and Wax Components

sample abbreviation	oligosaccharide	wax
MH-*b*-octacosane	maltoheptaose	octacosanol
MH-*b*-policosane	maltoheptaose	policosanol
β-CyD-*b*-policosane	betacyclodextrin	policosanol

naturally produced materials with no batch variability since the precursors (except policosanol whose chain length distribution can vary slightly by source) are chemically homogeneous. Although the molecular weights (ca. 1500 g/mol) of these naturally derived amphiphiles are not high enough to be strictly classified as polymers, they are indeed macromolecular architectures exhibiting self-assembly behavior similar to amphiphilic block copolymers.

MH and *β*-CyD were alkyne-functionalized using established procedures.[25,26] Octacosanol and policosanol were tosylated and then azide-functionalized using a procedure adapted from literature (Scheme 1a).[27] The azide-functionalized waxes were coupled to the alkyne-functionalized oligosaccharides on an approximately 1 g scale (Scheme 1b) following a similarly reported procedure.[23] Details on the synthesis procedures are reported in the Supporting Information.

The success of the wax functionalization was monitored by infrared spectroscopy (IR) and nuclear magnetic resonance (NMR), and the success of the coupling reaction was confirmed by IR (see Figures S1 and S2 in the Supporting Information). As evidenced by the complete disappearance of the azide peak in IR measurements after coupling, the wax was completely coupled to the oligosaccharide. Excess oligosaccharide was removed by precipitating in and washing with a mixture of water/methanol.

Studying the bulk self-assembly of these materials by thermal annealing alone is a challenge due to the strong hydrogen bonding and low degradation temperatures of the oligosaccharides.[6,23] Therefore, solvent vapor annealing was performed to drive microphase separation of block domains prior to a low-temperature thermal annealing step that removed solvent. Bulk MH-*b*-octacosane samples were solvent annealed in a tightly capped 125 mL jar (Fisher, catalog number 02–911–455) at room temperature for various times at atmospheric pressure. Within the jar was an uncapped 20 mL vial (Fisher, catalog number 03–337–15) filled with a mixture of 2.5 g tetrahydrofuran (THF) and 2.5 g water. The bulk self-assembly of the samples was investigated before and after solvent annealing by small-angle X-ray scattering (SAXS) data collected in vacuo (~0.3 Torr).

As-precipitated, a SAXS pattern was observed for MH-*b*-octacosane that is similar to as-precipitated samples of PTMSS-*b*-oligosaccharides studied previously,[23] characteristic of poorly

Scheme 1. (a) General Procedure for Azide-Functionalization of Waxes; (b) General Procedure for Oligosaccharide-Wax Coupling by Azide–Alkyne Cycloaddition

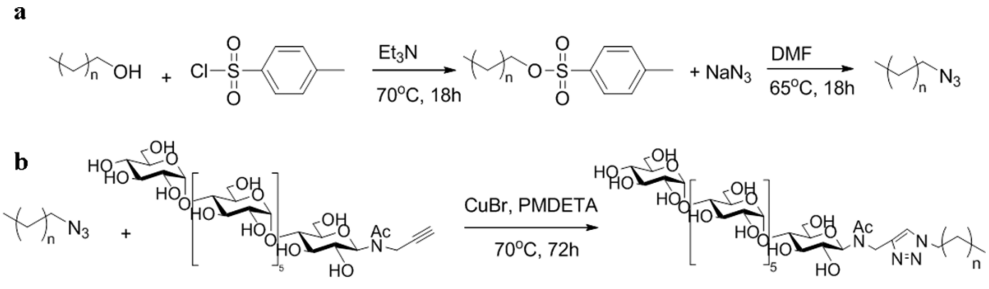

dx.doi.org/10.1021/mz500389g | ACS Macro Lett. 2014, 3, 839–844

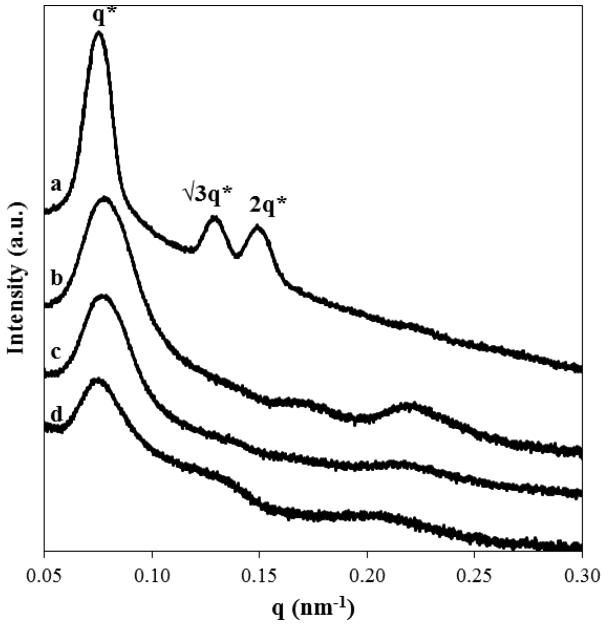

Figure 2. Evolution of SAXS patterns after solvent annealing/heating MH-*b*-octacosane. (a) After solvent vapor annealing for 48 h and heating to 160 °C for 30 min, (b) after only solvent vapor annealing for 48 h, (c) after only solvent vapor annealing for 24 h, and (d) as-precipitated. Curves are shifted vertically for clarity.

ordered micelles precipitated from the casting solution (Figure 2d). After solvent annealing in a jar with the 1:1 by mass mixture of THF and water, no improvement in order was observed after 24 or 48 h (Figure 2c,b, respectively). However, when the sample was heated to 160 °C for 30 min after solvent annealing, a relatively low temperature that precludes "caramelization" of sugar blocks,[6] higher-order scattering peaks consistent with a cylindrical morphology appeared (Figure 2a). The q^* peak is consistent with a domain periodicity, L_o, value of 8.4 nm, a remarkably small feature size that reflects their small block length and high chemical incompatibility between the blocks. The additional heating step likely removed residual water or THF solvent from the polymer after solvent vapor annealing, therefore, promoting self-assembly into highly ordered structures.

The self-assembly of the oligosaccharide-wax amphiphiles was also investigated in aqueous solution after preparation by nanoprecipitation, a commonly used polymersome formation technique.[28] The amphiphilic block oligomers were only slightly soluble in water (<0.1 mg/mL), probably due to the hydrophobic wax component. Compared with attempting to directly dissolve these oligomers in water, the following nanoprecipitation preparation method resulted in better dispersion of the oligomers in water, presumably due to reduced aggregation of the material by fully dissolving it in a good solvent first. A 1 mg aliquot of the block oligomer was dissolved in 2 mL of THF, and gentle heating was applied when necessary to fully dissolve the polymer. Next, the THF−polymer solution was added dropwise to 10 mL of water. The THF was removed by heating the solution to 90 °C for 15 min (above the boiling point of THF) and then pulling vacuum on the solution for about 15 min to remove any remaining THF. After removing the THF, some of the polymer precipitated from the water solution due to the low solubility of the block oligomer in water. These large particle aggregates were removed by filtering the solution through a 1 μm pore size PTFE filter. The preparation method used for the subsequent encapsulation experiments was identical (i.e., prepared by nanoprecipitation and filtration), except an additional 2 mg of the material to be encapsulated was added to the starting THF solution.

The particle size distribution of self-assembled colloids in aqueous solution was characterized by dynamic light scattering (DLS). As shown in Figure S4 of the Supporting Information, the autocorrelation functions for every sample tested decayed monotonically to zero at long delay times. As shown in Figure S5 of the Supporting Information, the CONTIN algorithm used

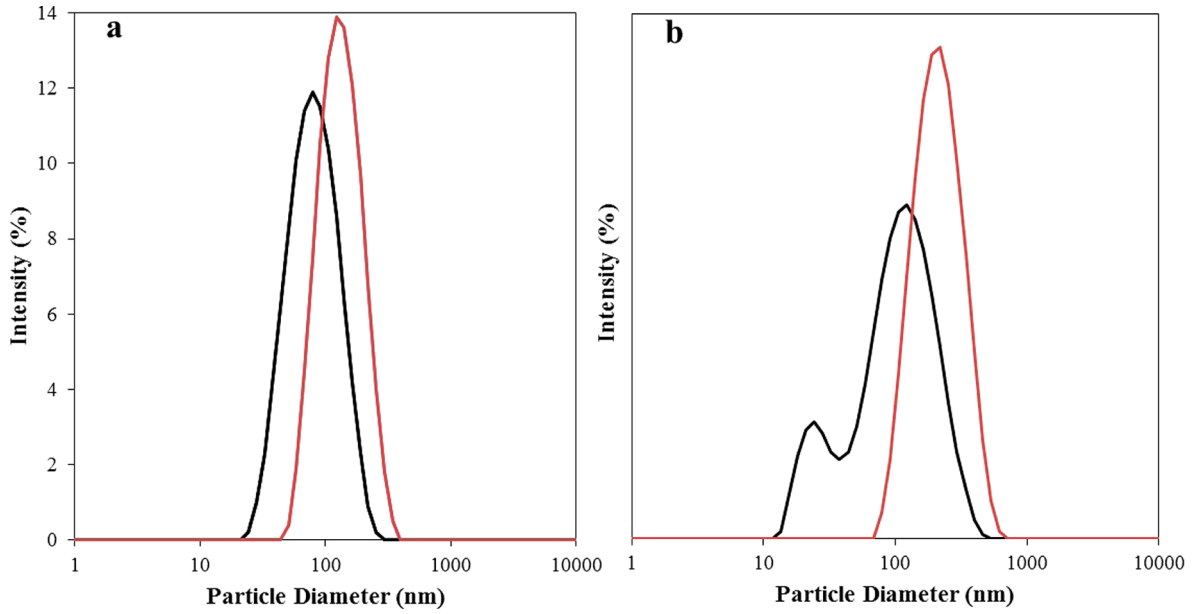

Figure 3. Size distribution curves obtained from DLS data. (a) Peak shift from MH-*b*-octacosane vesicles (black curve) to a larger particle diameter with encapsulated dotriacontane (red curve). (b) Peak shift from MH-*b*-policosane vesicles (black curve) to a larger particle diameter with encapsulated dotriacontane (red curve).

dx.doi.org/10.1021/mz500389g | *ACS Macro Lett.* 2014, 3, 839−844

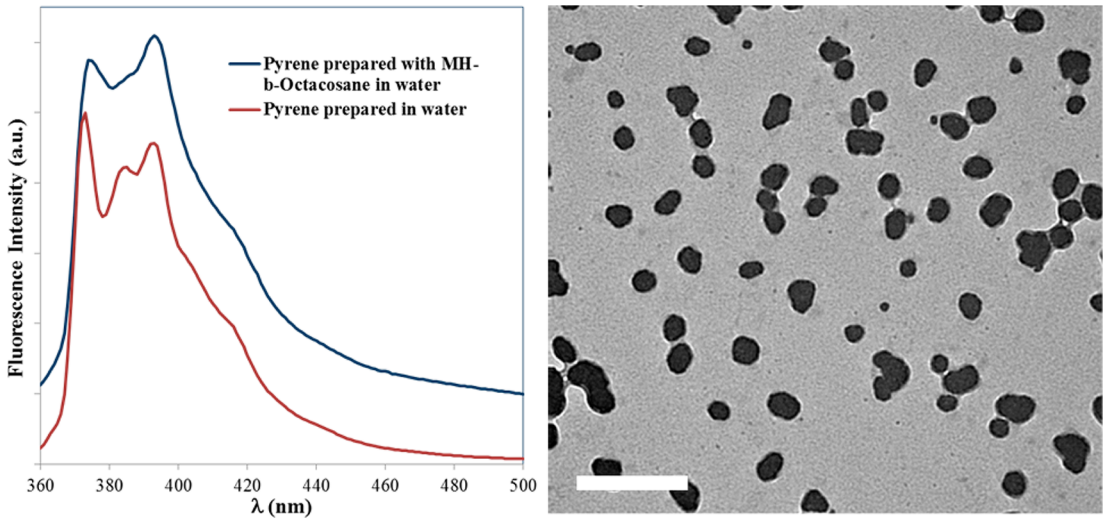

Figure 4. (Left) Normalized fluorescence emission spectra of pyrene in water and pyrene encapsulated within MH-*b*-octacosane vesicles. The excitation wavelength was 337 nm. Spectra are shifted vertically for clarity. (Right) TEM image of drop cast MH-*b*-octacosane vesicles after pyrene encapsulation with a particle diameter range of approximately 50−100 nm. The scale bar represents 400 nm.

by the instrument's software to deconvolute the correlation data and produce the size distribution curves always resulted in a high quality regression fit. The DLS particle size curve of MH-*b*-octacosane (Figure 3a) is monomodal and possesses a diameter of 80 nm at the peak of the distribution. This represents an unreasonably large diameter for a micelle structure, but is consistent with vesicle (bilayer) structures. DLS was also performed on MH-*b*-policosane (Figure 3b) and *β*-CyD-*b*-policosane. The size distribution curve obtained for MH-*b*-policosane was bimodal, indicating two different populations with diameters of 24 and 120 nm at the peak intensity values. The bimodal distribution was obtained for triplicate runs and represents the best fit to the DLS autocorrelation data, which appears stretched relative to the other samples. Since policosanol consists primarily of alkyl chains with a similar molecular weight to octacosanol, it was expected that a diameter similar to that of MH-*b*-octacosane would be obtained. Due to the polydispersity of the policosanol precursor, it is possible that the larger peak reflects vesicles formed from wax chain lengths, similar to the MH-*b*-octacosane, while the smaller peak arises from micelles or vesicles formed from shorter chain lengths. For the *β*-CyD-*b*-policosane, the scattered light fluctuations were uncorrelated (see Figure S6), indicating that a self-assembled structure is not present in aqueous solution. This could be due to the sterically hindered geometry of the *β*-CyD that prohibits micelle/vesicle formation, or the fact that *β*-CyD itself can encapsulate hydrophobic components such as the wax block.[29,30]

For therapeutic delivery applications, an ideal amphiphilic material should self-assemble into a micelle or vesicle structure, encapsulate a desired therapeutic component, and have desirable degradation or disassembly characteristics for component release.[31] In addition, ideal materials are nontoxic, so as not to disrupt biological functions while fulfilling functions as drug carriers, with predictable chain length distribution (perhaps by careful sourcing requirements) since there is concern that batch variation arising from chain length polydispersity could have an effect on the reproducibility in pharmaceutical applications of the materials.[32] We believe that these naturally derived amphiphiles would satisfy most of these five criteria.

The ability of the MH-*b*-octacosane to encapsulate a hydrophobic material was investigated. A relatively short chain hydrocarbon (short enough to be soluble in THF but long enough that it would be insoluble in water) dotriacontane was chosen as a model material to be encapsulated. Encapsulation was characterized by monitoring the diameter of the vesicles before and after encapsulation by DLS. The diameter at the peak of the distribution shifted from 80 nm for the unloaded vesicles to 122 nm for those with encapsulated dotriacontane, a notable size increase suggesting successful encapsulation of the dotriacontane (Figure 3a). We consider this result reasonable because other studies which compared sizes of drug-loaded vesicles to their unloaded analogs also report a similar size increase.[33,34] A similar increase in particle diameter was observed after encapsulating dotriacontane with MH-*b*-policosane (Figure 3b). The diameter at the peak of the distribution increases from 120 to 217 nm due to loading with dotriacontane. That the loaded sample has a monomodal distribution suggests that it has accommodated the fraction of MH-*b*-policosane which had formed small micelles/vesicles in the unloaded sample, perhaps due to its packing characteristics becoming more favorably incorporated into a larger diameter vesicle possessing lower curvature. The fact that the size distribution of the loaded MH-*b*-policosane vesicles is centered near 200 nm is of note because particles with sizes 100−300 nm concentrate in cancer tumors due to a size sieving effect present in tumor vasculature.[35,36]

To determine whether encapsulated hydrophobic molecules resided in the vesicle bilayer or in the aqueous environment inside the vesicle, a fluorescent probe molecule was encapsulated. This second hydrophobic component encapsulation was characterized by fluorescence spectroscopy using an excitation wavelength of 337 nm. We chose pyrene for this purpose because previous studies demonstrated that the fluorescence intensity ratios of the 373 and 383 nm peaks in the emission spectra are directly related to whether it is localized in a hydrophobic or hydrophilic environment.[37−39] If the ratio of the 373 to 383 nm peak is high (typically greater than 1 and less than 2), the pyrene is in a hydrophilic environment, and if it is lower (typically close-to or less-than 1), it is surrounded by a hydrophobic environment. Figure 4 shows the fluorescence emission spectra of pyrene in water and encapsulated in the vesicles, both normalized to the intensity at 373 nm and shifted vertically for clarity. In a water solution, prepared identically to the

dx.doi.org/10.1021/mz500389g | *ACS Macro Lett.* 2014, 3, 839−844

amphiphilic block oligomer solutions but without any oligomers, the emission intensity at 373 nm is much higher than that at the 383 nm peak (ratio = 1.2), indicating it is in a hydrophilic (aqueous) environment. In the solution with block oligomers added, the 373 nm peak is roughly the same as the 383 nm peak (i.e., the intensity ratio is 1.0), indicating that it is primarily in a hydrophobic environment (i.e., encapsulated within the vesicle bilayer and in contact with the wax). Removal of free, water solubilized pyrene could make the difference in peak heights more pronounced. However, since pyrene has very low solubility in water ($\sim 10^{-6}$ M), and the purpose of the study was to qualitatively illustrate the encapsulation of hydrophobic molecules, we did not attempt to remove the traces of free pyrene by dialysis before measurement.

Single-angle DLS provides information about the relative size of structures in solution (based on the assumption that the particles are spherical) but does not give information about the specific shape of the structures. The MH-*b*-octacosane solutions were imaged by transmission electron microscopy (TEM) with samples prepared by drop-casting on a TEM grid (i.e., depositing a drop of solution and then allowing the water to evaporate, leaving the vesicles behind). Most of the area on the TEM grid showed significant aggregation and very few isolated individual structures, from the concentration and subsequent precipitation of the amphiphilic oligomers upon water evaporation due to the low solubility of the block oligomers. Unfortunately, images of drop cast samples are not perfectly representative of the structure of their self-assembly in solution since changes in morphology and aggregation can occur during the solvent evaporation process. A technique like cryogenic TEM could be used to image structures in solution by imaging the solution in a vitrified state. Obtaining cryo-TEM images of the vesicles from this work was attempted; however, the aqueous amphiphile solutions reported herein were very dilute which made definitive identification of representative vesicles difficult to ascertain among ice crystals resulting from the sample preparation procedure. We anticipate if the sample was more concentrated it would be easier to distinguish vesicles from ice crystal artifacts. Figure S7 shows a representative micrograph of a water control sample (no block oligomers) in which many ice crystal artifacts are present.

However, pyrene-loaded vesicles could be imaged after drop casting the solution on a TEM grid (Figure 4). The fact that isolated structures could be imaged from a dried solution without forming significant aggregates suggests that the vesicles may be stabilized by the added pyrene, possibly by making the vesicle walls more rigid after loading. The particle diameters observed from drop cast imaging range from 50 to 100 nm. The drying procedure undoubtedly introduces some process artifacts which make direct comparisons of particle shape and size to the DLS sizes, measured in solution, inappropriate.

Three oligosaccharide-*b*-wax materials were synthesized through functionalization of the oligosaccharide and wax precursors and coupling by azide−alkyne cycloaddition. The self-assembly of the materials was investigated in the bulk by SAXS after solvent annealing and in aqueous solution by DLS and TEM. The amphiphilic block oligomers self-assembled into remarkably small cylindrical structures in the bulk after solvent annealing and heating. Successful vesicle formation and encapsulation of two different hydrophobic components was demonstrated by DLS and fluorescence spectroscopy. The ability of these biocompatible materials to self-assemble in bulk and solution and encapsulate hydrophobic materials makes them attractive candidates for further studies in therapeutic delivery applications.

■ ASSOCIATED CONTENT

Supporting Information

Synthesis and characterization details. This material is available free of charge via the Internet at http://pubs.acs.org.

■ AUTHOR INFORMATION

Corresponding Author

*Phone: 512-471-6300. E-mail: ellison@che.utexas.edu.

Notes

The authors declare no competing financial interest.

■ ACKNOWLEDGMENTS

The authors thank Nissan Chemical Company for financial support. C. Ellison thanks the Welch Foundation (Grant #F-1709) for partial financial support. This work was also supported by the National Science Foundation through a Graduate Research Fellowship to J. Cushen. The authors thank Joseph Lott from the University of Minnesota for providing assistance with cryo TEM experiments. Cryo TEM experiments were financially supported in part by the National Science Foundation through the University of Minnesota MRSEC under Award Number DMR-0819885. SAXS and DLS were performed at the Center for Nano- and Molecular Science/Texas Materials Institute.

■ REFERENCES

(1) Jorfi, M.; Roberts, M. N.; Foster, E. J.; Weder, C. *ACS Appl. Mater. Interfaces* **2013**, *5*, 1517−1526.
(2) Johnson, J. C.; Korley, L. T. J. *Soft Matter* **2012**, *8*, 11431−11442.
(3) Zhong, C.; Deng, Y.; Roudsari, A. F.; Kapetanovic, A.; Anantram, M. P.; Rolandi, M. *Nat. Commun.* **2011**, *2*, 476.
(4) Williams, C. K.; Hillmyer, M. A. *Polym. Rev.* **2008**, *48*, 1−10.
(5) Isono, T.; Otsuka, I.; Suemasa, D.; Rochas, C.; Satoh, T.; Borsali, R.; Kakuchi, T. *Macromolecules* **2013**, *46*, 8932−8940.
(6) Otsuka, I.; Isono, T.; Rochas, C.; Halila, S.; Fort, S.; Satoh, T.; Kakuchi, T.; Borsali, R. *ACS Macro Lett.* **2012**, *1*, 1379−1382.
(7) Kataoka, K.; Harada, A.; Nagasaki, Y. *Adv. Drug Delivery Rev.* **2012**, *64* (Supplement), 37−48.
(8) Kazunori, K.; Glenn S, K.; Masayuki, Y.; Teruo, O.; Yasuhisa, S. *J. Controlled Release* **1993**, *24*, 119−132.
(9) Xiong, X.-B.; Falamarzian, A.; Garg, S. M.; Lavasanifar, A. *J. Controlled Release* **2011**, *155*, 248−261.
(10) Alexandridis, P.; Lindman, B. *Amphiphilic block copolymers: self-assembly and applications*; Elsevier: New York, 2000.
(11) Discher, B. M.; Won, Y.-Y.; Ege, D. S.; Lee, J. C.-M.; Bates, F. S.; Discher, D. E.; Hammer, D. A. *Science* **1999**, *284*, 1143−1146.
(12) Huang, J.; Bonduelle, C.; Thévenot, J.; Lecommandoux, S.; Heise, A. *J. Am. Chem. Soc.* **2011**, *134*, 119−122.
(13) Israelachvili, J. N.; Mitchell, D. J.; Ninham, B. W. *Biochim. Biophys. Acta, Biomembr.* **1977**, *470*, 185−201.
(14) Xiong, X.-B.; Binkhathlan, Z.; Molavi, O.; Lavasanifar, A. *Acta Biomater.* **2012**, *8*, 2017−2033.
(15) Yang, S.-J.; Lee, H.-S.; Kim, J.-W.; Lee, M.-H.; Auh, J.-H.; Lee, B.-H.; Park, K.-H. *Carbohydr. Res.* **2006**, *341*, 420−424.
(16) Biwer, A.; Antranikian, G.; Heinzle, E. *Appl. Microbiol. Biotechnol.* **2002**, *59*, 609−617.
(17) Jansen, T.; Xhonneux, B.; Mesens, J.; Borgers, M. *Lens Eye Toxicity Res.* **1990**, *7*, 459−468.
(18) Astray, G.; Gonzalez-Barreiro, C.; Mejuto, J. C.; Rial-Otero, R.; Simal-Gándara, J. *Food Hydrocolloids* **2009**, *23*, 1631−1640.
(19) Irmak, S.; Dunford, N. T.; Milligan, J. *Food Chem.* **2006**, *95*, 312−318.

(20) Chen, F.; Cai, T.; Zhao, G.; Liao, X.; Guo, L.; Hu, X. *J. Food Eng.* **2005**, *70*, 47−53.
(21) Kato, S.; Karino, K.-I.; Hasegawa, S.; Nagasawa, J.; Nagasaki, A.; Eguchi, M.; Ichinose, T.; Tago, K.; Okumori, H.; Hamatani, K.; Takahashi, M.; Ogasawara, J.; Masushige, S. *Br. J. Nutr.* **1995**, *73*, 433−441.
(22) Janikula, M. *Policosanol: A new treatment for cardiovascular disease*? Alternative Medicine Review; ETATS-UNIS: Dover, ID, 2002; Vol. 7, p 15.
(23) Cushen, J. D.; Otsuka, I.; Bates, C. M.; Halila, S.; Fort, S.; Rochas, C.; Easley, J. A.; Rausch, E. L.; Thio, A.; Borsali, R.; Willson, C. G.; Ellison, C. J. *ACS Nano* **2012**, *6*, 3424−3433.
(24) Aissou, K. A. K.; Otsuka, I.; Rochas, C.; Fort, S.; Halila, S.; Borsali, R. *Langmuir* **2011**, *27*, 4098−4103.
(25) Otsuka, I.; Fuchise, K.; Halila, S.; Fort, S. b.; Aissou, K.; Pignot-Paintrand, I.; Chen, Y.; Narumi, A.; Kakuchi, T.; Borsali, R. *Langmuir* **2009**, *26*, 2325−2332.
(26) Guo, Z.; Jin, Y.; Liang, T.; Liu, Y.; Xu, Q.; Liang, X.; Lei, A. *J. Chromatogr., A* **2009**, *1216*, 257−263.
(27) Link, A. J.; Vink, M. K. S.; Tirrell, D. A. *Nat. Protocols* **2007**, *2*, 1884−1887.
(28) Fessi, H.; Puisieux, F.; Devissaguet, J. P.; Ammoury, N.; Benita, S. *Int. J. Pharm.* **1989**, *55*, R1−R4.
(29) Rimmer, S.; Tattersall, P. I. *Polymer* **1999**, *40*, 6673−6677.
(30) Leyrer, R. J.; Mächtle, W. *Macromol. Chem. Phys.* **2000**, *201*, 1235−1243.
(31) Shuai, X.; Ai, H.; Nasongkla, N.; Kim, S.; Gao, J. *J. Controlled Release* **2004**, *98*, 415−426.
(32) Porter, C. J. H.; Moghimi, S. M.; Davies, M. C.; Davis, S. S.; Illum, L. *Int. J. Pharm.* **1992**, *83*, 273−276.
(33) Girhepunje, K.; Pal, R.; Behera, A.; Husen, M.; Thirumoorthy, N. *J. Pharm. Res.* **2010**, *3*, 2898−2900.
(34) Shaik, H. R.; Tirumooorthy, N.; Girhepunje, K. *World J. Pharm. Pharm. Sci.* **2012**, *1*, 280−289.
(35) Ungun, B.; Prud'homme, R. K.; Budijon, S. J.; Shan, J.; Lim, S. F.; Ju, Y.; Austin, R. *Opt. Express* **2009**, *17*, 80−86.
(36) Torchilin, V. P.; Trubetskoy, V. S. *Adv. Drug Delivery Rev.* **1995**, *16*, 141−155.
(37) Basu Ray, G.; Chakraborty, I.; Moulik, S. P. *J. Colloid Interface Sci.* **2006**, *294*, 248−254.
(38) Topel, Ö.; Çakır, B. A.; Budama, L.; Hoda, N. *J. Mol. Liq.* **2013**, *177*, 40−43.
(39) Turro, N. J.; Kuo, P. L.; Somasundaran, P.; Wong, K. *J. Phys. Chem.* **1986**, *90*, 288−291.